POLITECNICO DI TORINO
Repository ISTITUZIONALE

Free space optical system performance for laser beam propagation through non Kolmogorov turbulence for uplink and downlink paths

Original
Free space optical system performance for laser beam propagation through non Kolmogorov turbulence for uplink and downlink paths / Italo, T., LARRY C., A., RONALD L., P., Ferrero, V.. - STAMPA. - 6708:(2007), pp. 670803-1-670803-12. (SPIE: Atmospheric Optics: Models, Measurements, and Target-in-the-Loop Propagation San Diego, California August 2007) [10.1117/12.732595].

Availability:
This version is available at: 11583/1995697 since: 2016-11-04T13:40:17Z

Publisher:

Published
DOI:10.1117/12.732595

Terms of use:

This article is made available under terms and conditions as specified in the corresponding bibliographic description in the repository

Publisher copyright

(Article begins on next page)

29 June 2026

Free space optical system performance for laser beam propagation through non Kolmogorov turbulence for uplink and downlink paths

Italo Toselli[a], Larry. C. Andrews[b], Ronald L. Phillips[c], Valter Ferrero[a]

[a]Optical Communications Group, Politecnico di Torino, 10128 Turin, Italy
[b]Department of Mathematics, University of Central Florida, Orlando, FL32816
[c]University of Central Florida, Space Institute, MS: FSI, Kennedy Space Center, Florida 32899

ABSTRACT

It is well known that free space laser system performance is limited by atmospheric turbulence. Most theoretical treatments have been described for many years by Kolmogorov's power spectral density model because of its simplicity. Unfortunately several experiments have been reported recently that show the Kolmogorov theory is sometimes incomplete to describe atmospheric statistics properly, in particular, in portions of the troposphere and stratosphere. In this paper, using a non Kolmogorov spectrum and following same procedure already used for horizontal path analysis, we extend free space optical system performance analysis to uplink and downlink paths. Our non Kolmogorov spectrum uses a generalized exponent instead of constant standard exponent value 11/3 and a generalized amplitude factor instead of constant value 0.033. Therefore, in non-Kolmogorov weak turbulence, we carry out, for a uplink and a downlink paths, analysis of Long Term Beam Spread, Scintillation index, Probability of fade, mean SNR and mean BER as variation of the spectrum exponent.

Keywords: Atmospheric turbulence, structure function, Kolmogorov spectrum, non Kolmogorov spectrum, beam spread, scintillation, fade, SNR, BER, uplink, downlink.

1. INTRODUCTION

Since it has been introduced Kolmogorov's power spectral density model has been widely used and accepted to describe wave propagation through atmospheric turbulence. It has been already used also to calculate free space laser system performance that is limited by atmospheric turbulence. However, recent experimental data from space-based stellar scintillation, balloon-borne in-situ temperature, and ground-based radar measurements indicate turbulence in the upper troposphere and stratosphere deviates from predictions of the Kolmogorov model [5][9][10]. Further development of the turbulent theory of passive scalar transfer has shown that although the Kolmogorov spectrum is important, it constitutes only one part of the more general behavior of passive scalar transfer in a turbulent flow [6]. Some anomaly behavior [3] seem to occur when the atmosphere is extremely stable because under such condition the turbulence is no longer homogeneous in three dimensions since the vertical component is suppressed. It has been shown [4] that for such two dimensional turbulence, coherent vortices can develop that reduce rate of the energy cascade from larger to smaller scales. As a result Kolmogorov turbulence will not develop. In addition anisotropy in stratospheric turbulent inhomogeneities has been experimentally investigated [5][8][11][12]. We must accept de facto that turbulence is still an unsolved problem in classical physics and the scientific community must persist in doing more simulations, measurements and experiments [7].
It is very important, therefore, to find new models more general than Kolmogorov spectrum in order to describe also non Kolmogorov turbulence. In this paper we present a theoretical spectrum model which reduces to one of Kolmogorov only for a particular case of its exponent: the standard value 11/3. Exponent can assume all the values between the range 3 to 4. Using this new spectrum, following the same procedure already used from Andrews and Phillips [1][2], we have analyzed the impact of the exponent's variation on *Long Term Beam Spread, Scintillation index, Probability of fade, mean Signal to Noise Ratio (SNR)* and *Mean Bit Error Rate (BER)* for uplink and downlink paths. Horizontal link has been already analyzed in [13].

Atmospheric Optics: Models, Measurements, and Target-in-the-Loop Propagation,
edited by Stephen M. Hammel, Alexander M. J. van Eijk, Michael T. Valley, Mikhail A. Vorontsov,
Proc. of SPIE Vol. 6708, 670803, (2007) · 0277-786X/07/$18 · doi: 10.1117/12.732595

2. NON KOLMOGOROV SPECTRUM

We assume that in an atmosphere exhibiting non-Kolmogorov turbulence the structure function for the index of refraction is given by [1][13]

$$D_n(r) = \beta \cdot C_n^2 \cdot r^{\gamma} \tag{1}$$

where γ is the power law which reduces to 2/3 in the case of conventional Kolmogorov turbulence. Here, β is a constant equal to unity when $\gamma = 2/3$, but otherwise has units $\mathrm{m}^{-\gamma+2/3}$. The corresponding power-law spectrum associated with structure function, as reported in [1][13], takes the form

$$\Phi_n(\kappa,\alpha) = A(\alpha)\cdot \tilde{C}_n^2 \cdot \kappa^{-\alpha}, \quad \kappa > 0,\ 3 < \alpha < 4, \tag{2}$$

where $\alpha = \gamma + 3$ is the spectral index or power law, $\tilde{C}_n^2 = \beta \cdot C_n^2$ is a generalized structure parameter with units $\mathrm{m}^{-\gamma}$, $A(\alpha)$ is defined by

$$A(\alpha) = \frac{1}{4\pi^2}\Gamma(\alpha-1)\cos\left(\frac{\alpha\pi}{2}\right), \quad 3 < \alpha < 4. \tag{3}$$

the symbol $\Gamma(x)$ in the last expression is the gamma function. When $\alpha = 11/3$, we find that $A(11/3) = 0.033$ and the generalized power spectrum reduces to the conventional Kolmogorov spectrum. Also, when the power law approaches the limiting value $\alpha = 3$, the function $A(\alpha)$ approaches zero. Consequently, the refractive-index power spectral density vanishes in this limiting case.

3. LONG TERM BEAM SPREAD

The analytical form of *Long Term Beam Spread* for a Gaussian beam wave is [1]

$$W_e^2 = \left\langle W_{LT}^2(\alpha)\right\rangle = W^2 \cdot \left[1 + \left\langle T(\alpha)\right\rangle\right] \tag{4}$$

where W is the diffraction limited spot size radius and $\left\langle T(\alpha)\right\rangle$ is the term which includes small scale beam spreading and beam wander atmospheric effects. In order to carry out Long Term Beam Spread analysis we need to calculate the $\left\langle T(\alpha)\right\rangle$ term both for uplink and downlink. A horizontal link has been analyzed in [13].

For slant paths, the parameter C_n^2 that appears inside the relation $\tilde{C}_n^2 = \beta \cdot C_n^2$ is not constant, but it changes with altitude. Utilizing the Hufnagle-Valley $C_n^2(h)$ profile model and following the same procedure of Andrews and Phillips [1] but using the non Kolmogorov spectrum, we carry out

$$T(\alpha) = 4\pi^2 k^2 \cdot \left(\int_0^L \int_0^{\infty} \kappa \cdot \phi_n(\alpha,\kappa,z)\left[1 - \exp\left(-\frac{\Lambda L \kappa^2 \left(1-\frac{z}{L}\right)^2}{k}\right)\right] d\kappa dz \right) \tag{5}$$

$$= -2\pi^2 \cdot A(\alpha)\cdot \Gamma\left(1-\frac{\alpha}{2}\right)\cdot k^{3-\frac{\alpha}{2}} \Lambda^{\frac{\alpha}{2}-1} \cdot L^{\frac{\alpha}{2}-1} \cdot \int_0^L \tilde{C}_n^2(z)\cdot\left(1-\frac{z}{L}\right)^{\alpha-2} dz$$

where z is the propagation distance and $\Lambda = 2L/kW^2$.

In particular for downlink and uplink paths, introducing zenith angle ζ that is the angle between satellite-ground station axis and the normal respect to the ground, h_0 that is the height above ground level of uplink transmitter and/or downlink receiver and H that is satellite altitude, it is easy to carry out

$$T(\alpha)_{downlink} = -2\pi^2 \cdot A(\alpha) \cdot \Gamma\left(1-\frac{\alpha}{2}\right) \cdot k^{3-\frac{\alpha}{2}} \Lambda^{\frac{\alpha}{2}-1} \cdot (H-h_0)^{\frac{\alpha}{2}-1} \cdot \left[\sec(\zeta)\right]^{\frac{\alpha}{2}} \int_{h_0}^{H} \tilde{C}_n^2(h) \cdot \left(\frac{h-h_0}{H-h_0}\right)^{\alpha-2} dh \qquad (6)$$

$$T(\alpha)_{up\_link} = -2\pi^2 \cdot A(\alpha) \cdot \Gamma\left(1-\frac{\alpha}{2}\right) \cdot k^{3-\frac{\alpha}{2}} \Lambda^{\frac{\alpha}{2}-1} \cdot (H-h_0)^{\frac{\alpha}{2}-1} \cdot \left[\sec(\zeta)\right]^{\frac{\alpha}{2}} \int_{h_0}^{H} \tilde{C}_n^2(h) \cdot \left(1-\frac{h-h_0}{H-h_0}\right)^{\alpha-2} dh \qquad (7)$$

At this point, we plot in figure 1 the $T(\alpha)$ term as a function of alpha for uplink and downlink using two different W_0 values . We take: $H = 350km; \tilde{C}_n^2(0) = 7 \cdot 10^{-14}\, m^{-\alpha+3}; \lambda = 1.55\mu m; \zeta = 0, h_0 = 0$.

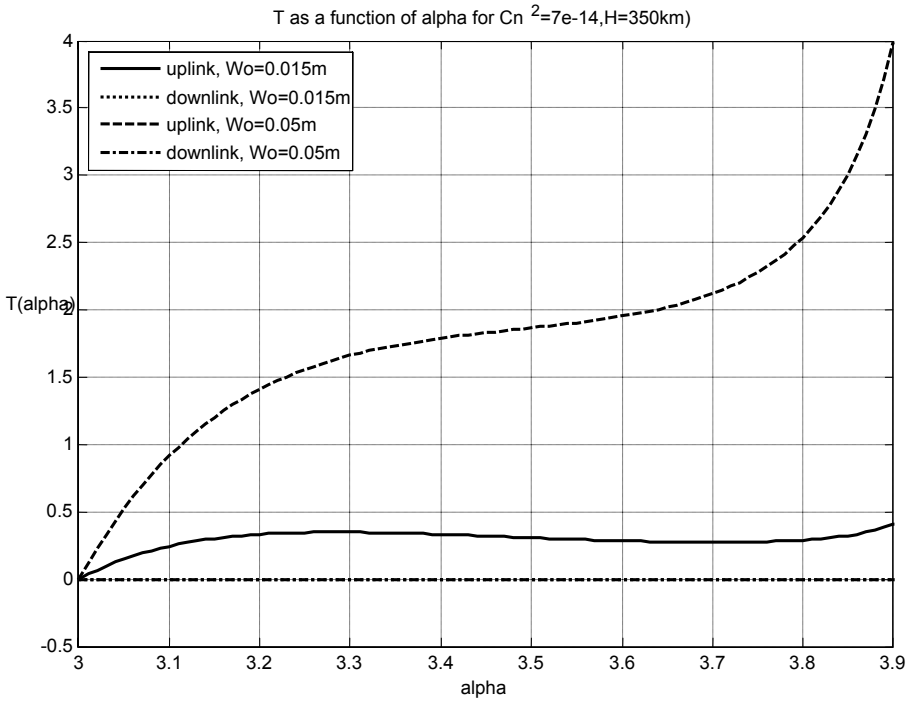

Figure 1- T(alpha) as a function of alpha for uplink and downlink paths

We deduce from figure 1 that, for uplink path, the slopes of the curves remarkable depends not only from alpha but also from the W_0 value. In fact, for $W_0 = 0.05m$, if alpha decreases from Kolmogorov value $\alpha = 11/3$, then $T(\alpha)$ decreases. In particular, for $\alpha = 3$, $T(\alpha)$ approaches zero because the term $A(\alpha)$ assumes null value and the long term beam spread W_e approaches the diffraction limited spot size radius. We deduce also that, if alpha increases from $\alpha = 11/3$, then the $T(\alpha)$ increases. The rise of the curve is more remarkable close to $\alpha = 4$ because the term

$\Gamma\left(1-\frac{\alpha}{2}\right)$ assumes high values close to its asymptote. However, for lower W_0, for instance $W_0 = 0.015m$, the slope of the curve is different. In fact, if alpha decreases from $\alpha = 11/3$ then $T(\alpha)$ increases up to a maximum value. At this point the curve changes its slope because of the term $A(\alpha)$ that assumes very low values. However, if alpha increases from $\alpha = 11/3$ then $T(\alpha)$ decreases down to a minimum value. At this point the curve changes its slope because of the term $\Gamma\left(1-\frac{\alpha}{2}\right)$ that assumes high values close to its asymptote.
For downlink path we do not have long term beam spread, but this was predictable because in downlink case the beam does not spread beyond that for diffraction [1].

4. SCINTILLATION INDEX

An important parameter that is necessary in order to calculate the system performance is the scintillation index. In our analysis we include aperture averaging effects of the receiver aperture, so we carry out the flux variance in the plane of the detector of diameter D_G. In addition, we will use the scintillation index of plane wave for the downlink case and the scintillation index of a spherical wave for the uplink case. We presume very similar results with respect to Gaussian scintillation index [1]. Finally, in our analysis we assume that beam wander induced scintillation is negligible which is true when we consider either a plane wave or a spherical wave, but the situation may be different for focused beams [1].

4.1 Downlink: plane wave model

In this case the parameter C_n^2 that appears inside the realation $\tilde{C}_n^2 = \beta \cdot C_n^2$ is not constant, but it changes with altitude. Utilizing the Hufnagle-Valley $C_n^2(h)$ profile model and following the same procedure of Andrews and Phillips [1] but this time using a non Kolmogorov spectrum, we obtain for plane wave model

$$\sigma_{I\_plane}^2(D_G) = 8\pi^2 \cdot k^2 \cdot \mathrm{Re}\left\{\int_0^L \int_0^\infty \kappa \cdot \Phi_n(\kappa,\alpha,z) \cdot \exp\left(-\frac{D_G^2 \cdot \kappa^2}{16}\right) \cdot \left[1-\exp\left(-j\frac{L\cdot\kappa^2\cdot\left(1-\frac{z}{L}\right)}{k}\right)\right] d\kappa dz\right\}$$

$$= 4\pi^2 \cdot k^2 \cdot A(\alpha) \cdot \left(\frac{16}{D_G^2}\right)^{1-\frac{\alpha}{2}} \cdot \Gamma\left(1-\frac{\alpha}{2}\right) \cdot \tag{8}$$

$$\times \int_0^L \tilde{C}_n^2(z) \left\{1-\left[\frac{16\cdot L\cdot\left(1-\frac{z}{L}\right)}{k\cdot D_G^2}\right]^{\frac{\alpha}{2}-1} \cdot \left[\left(\frac{k\cdot D_G^2}{16\cdot L\cdot\left(1-\frac{z}{L}\right)}\right)^2+1\right]^{\frac{1}{2}\left(\frac{\alpha}{2}-1\right)} \cdot \cos\left[\left(\frac{\alpha}{2}-1\right)\cdot arctg\left(\frac{16\cdot L\cdot\left(1-\frac{z}{L}\right)}{k\cdot D_G^2}\right)\right]\right\} dz$$

in particular, for downlink we obtain

$$\sigma^2_{I\_plane}\left(D_G\right)=4\pi^2\cdot k^2\cdot A(\alpha).\left(\frac{16}{D_G^2}\right)^{1-\frac{\alpha}{2}}\cdot\Gamma\left(1-\frac{\alpha}{2}\right)\cdot\sec(\varsigma)\cdot$$

$$\times\int_{h0}^{H}\tilde{C}_n^2(h)\left\{1-\left[\frac{16\cdot\frac{h-h_0}{\cos(\varsigma)}}{k\cdot D_G^2}\right]^{\frac{\alpha}{2}-1}\cdot\left[\left(\frac{k\cdot D_G^2}{16\cdot\frac{h-h_0}{\cos(\varsigma)}}\right)^2+1\right]^{\frac{1}{2}\left(\frac{\alpha}{2}-1\right)}\cdot\cos\left[\left(\frac{\alpha}{2}-1\right)\cdot arctg\left(\frac{16\cdot\frac{h-h_0}{\cos(\varsigma)}}{k\cdot D_G^2}\right)\right]\right\}dh \quad (9)$$

4.2 Uplink: spherical wave model

In this case the parameter C_n^2 that appears inside the realation $\tilde{C}_n^2=\beta\cdot C_n^2$ is not constant, but it changes with altitude. Utilizing the Hufnagle-Valley $C_n^2(h)$ profile model and following the same procedure of Andrews and Phillips [1] but this time using a non Kolmogorov spectrum, we obtain for spherical wave model

$$\sigma^2_{I\_spherical}\left(D_G\right)=8\pi^2\cdot k^2\cdot\mathrm{Re}\left\{\int_0^L\int_0^\infty\kappa\cdot\Phi_n(\kappa,\alpha)\cdot\exp\left(-\frac{D_G^2\cdot\kappa^2\cdot\left(1-\frac{z}{L}\right)^2}{16}\right)\cdot\left[1-\exp\left(-j\frac{L\cdot\kappa^2\cdot\left(1-\frac{z}{L}\right)\cdot\frac{z}{L}}{k}\right)\right]d\kappa d\xi\right\}$$

$$=4\pi^2\cdot k^2\cdot A(\alpha)\cdot\left(\frac{16}{D_G^2}\right)^{1-\frac{\alpha}{2}}\cdot\Gamma\left(1-\frac{\alpha}{2}\right)\cdot\left\{\int_0^L\tilde{C}_n^2(z)\cdot\left(1-\frac{z}{L}\right)^{\alpha-2}dz-\mathrm{Re}\left\{\int_0^L\tilde{C}_n^2(z)\cdot\left(\left(1-\frac{z}{L}\right)^2+j\frac{16\cdot\left(1-\frac{z}{L}\right)\cdot z}{k\cdot D_G^2}\right)^{\frac{\alpha}{2}-1}dz\right\}\right\} \quad (10)$$

in particular, for uplink we obtain

$$\sigma^2_{I\_spherical}\left(D_G\right)=4\pi^2\cdot k^2\cdot A(\alpha)\cdot\left(\frac{16}{D_G^2}\right)^{1-\frac{\alpha}{2}}\cdot\Gamma\left(1-\frac{\alpha}{2}\right)\cdot\sec(\varsigma)\cdot$$

$$\times\left\{\int_{h_0}^{H}\tilde{C}_n^2(h)\cdot\left(1-\frac{h-h_0}{H-h_0}\right)^{\alpha-2}dh-\mathrm{Re}\left\{\int_{h_0}^{H}\tilde{C}_n^2(h)\cdot\left(\left(1-\frac{h-h_0}{H-h_0}\right)^2+j\frac{16\cdot\left(1-\frac{h-h_0}{H-h_0}\right)\cdot\frac{h-h_0}{\cos(\varsigma)}}{k\cdot D_G^2}\right)^{\frac{\alpha}{2}-1}dh\right\}\right\} \quad (11)$$

At this point, we plot both $\sigma^2_{I\_plane}\left(D_G\right)$ and $\sigma^2_{I\_spherical}\left(D_G\right)$ as a function of alpha respectively for downlink and uplink case. We take

$H=350km;h_0=0;\varsigma=0;\tilde{C}_n^2(0)=7\cdot10^{-14}\,m^{-\alpha+3};\lambda=1.55\mu m;D_G=0.1m.$

The results are shown in figure 2.

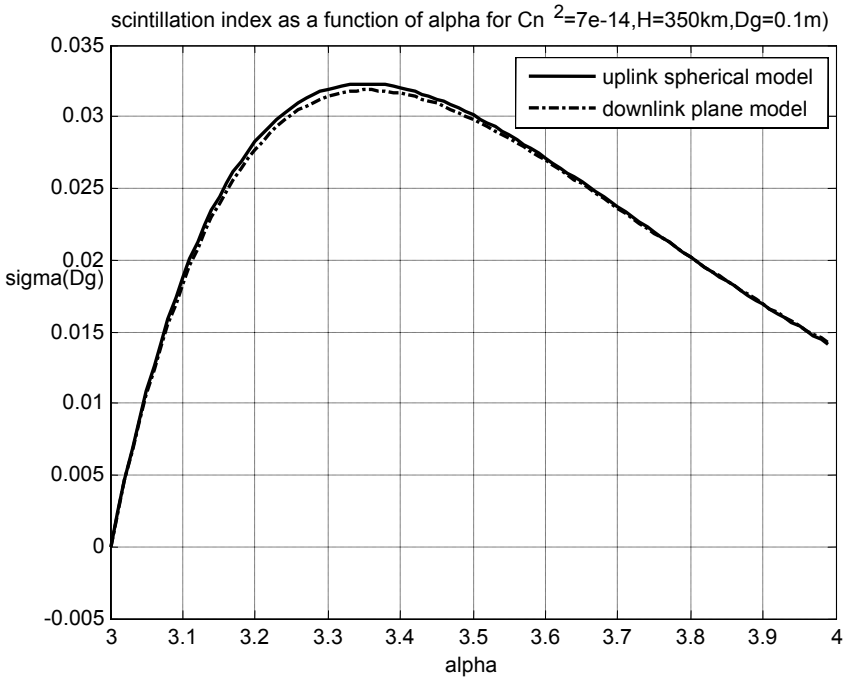

Figure 2- Scintillation index as a function of alpha for uplink and downlink paths

We deduce from figure 2 that for alpha values lower than Kolmogorov value $\alpha = 11/3$ there is an increase of scintillation both for the spherical wave model (uplink) and the plane wave model (downlink). Consequently scintillation in this case leads to a penalty on the system performance. We deduce also that there are two maximum values of scintillation around the same alpha values close to 3.35. At this point the curves change their slopes because the term $A(\alpha)$ begins to decrease to zero. In addition for alpha values higher than $\alpha = 11/3$, scintillation slightly decreases for both the plane wave model and spherical wave model and consequently it will lead to a slight gain on the system performance.

5 PROBABILITY OF FADE

Given a PDF model for irradiance fluctuations $p_I(I)$, the probability of fade describes the percentage of time the irradiance of the received signal is below some prescribed threshold value I_T. Hence, the probability of fade as a function of threshold level is defined by the cumulative probability [1]

$$p_I(I < I_T) = \int_0^{I_T} p_I(I)\, dI \tag{12}$$

The PDF most often used under weak irradiance fluctuations is the lognormal model and the resulting probability of fade leads to

$$p_I(I < I_T) = \frac{1}{2} \cdot \left\{ 1 + erf\left[\frac{\frac{1}{2} \cdot \sigma_I^2(\alpha, D_G) - 0.23 \cdot F_T}{\sqrt{2} \cdot \sigma_I(\alpha, D_G)} \right] \right\}, \tag{13}$$

where $erf(x)$ is the error function, and F_T is the fade threshold parameter, given in decibels $[dB]$, which represents the dB level below the on-axis mean irradiance that the threshold is set [1].

5.1 Downlink: plane wave model

Using the plane wave model scintillation index (9), we plot the Probability of Fade as a function of alpha and a fixed fade threshold parameter for a particular downlink case in which

$$H = 350km; h_0 = 0; \varsigma = 0; \tilde{C}_n^2(0) = 7 \cdot 10^{-14} m^{-\alpha+3}; \lambda = 1.55\mu m; D_G = 0.2m; Ft = 3dB$$

The plot is shown in figure 3.

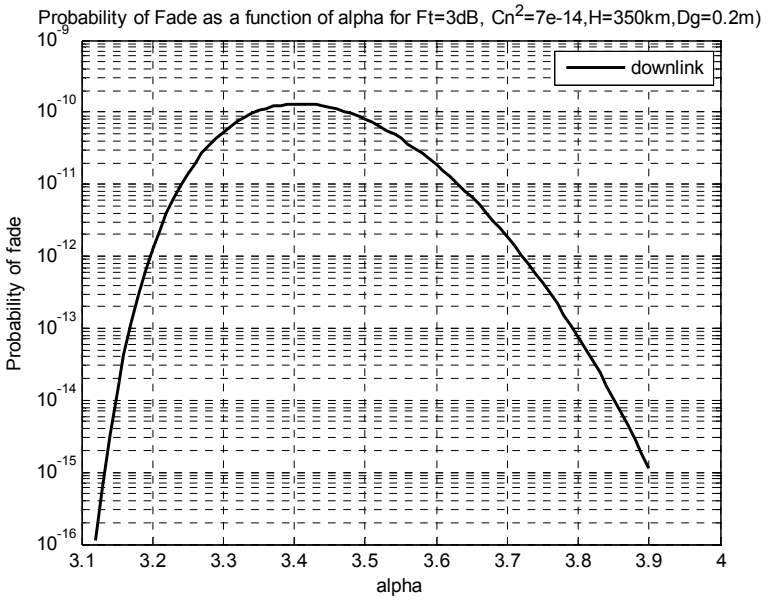

Figure 3- Probability of fade as a function of alpha for downlink path

5.2 Uplink: spherical wave model

Using the spherical wave model scintillation index (11), we plot the Probability of Fade as a function of alpha and a fixed fade threshold parameter for a particular uplink case in which

$$H = 350km; h_0 = 0; \varsigma = 0; \tilde{C}_n^2(0) = 7 \cdot 10^{-14} m^{-\alpha+3}; \lambda = 1.55\mu m; D_G = 0.1m; Ft = 3dB$$

The plot is shown in figure 4.

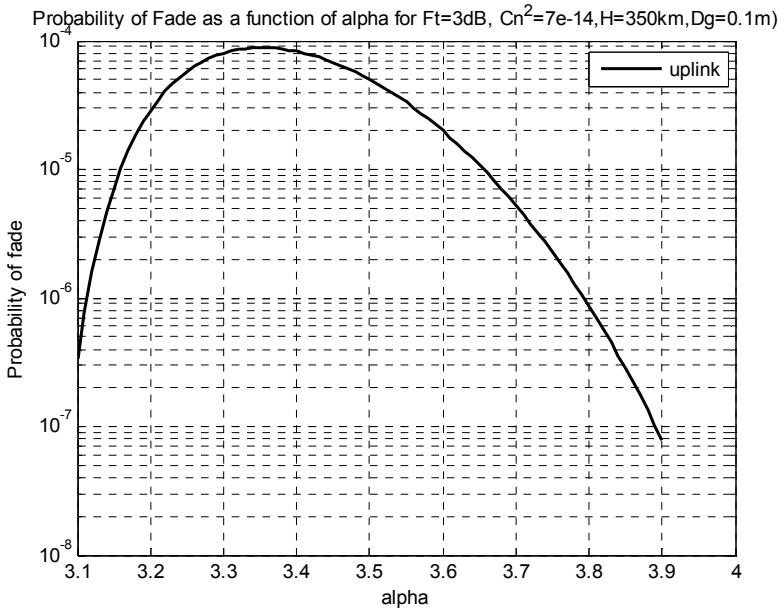

Figure 4- Probability of fade as a function of alpha for uplink path

6. MEAN SIGNAL TO NOISE RATIO

In this section we examine the *Mean Signal to Noise Ratio* in the presence of atmospheric turbulence using a non Kolmogorov power spectrum. The received irradiance over long measurement intervals must be treated like a random variable because of the turbulence.

Based on [1][2], the mean Signal to Noise Ratio $\langle SNR \rangle$ at the output of the detector in the case of a shot-noise limited system assumes the form

$$\langle SNR \rangle = \frac{SNR_0}{\sqrt{1+\sigma_I^2(\alpha, D_G)\cdot SNR_0{}^2}} \tag{14}$$

where SNR_0 is the signal to noise ratio in the absence of turbulence.

6.1 Downlink: plane wave model

We plot in dB units the Mean Signal to Noise Ratio as a function of the signal to noise ratio without turbulence for several alpha values and using the plane wave model for scintillation (9).
We take follow parameters

$$H = 350km; h_0 = 0; \varsigma = 0; \tilde{C}_n^2(0) = 7\cdot 10^{-14}\, m^{-\alpha+3}; \lambda = 1.55\mu m; D_G = 0.2m.$$

The plot is shown in figure 5.

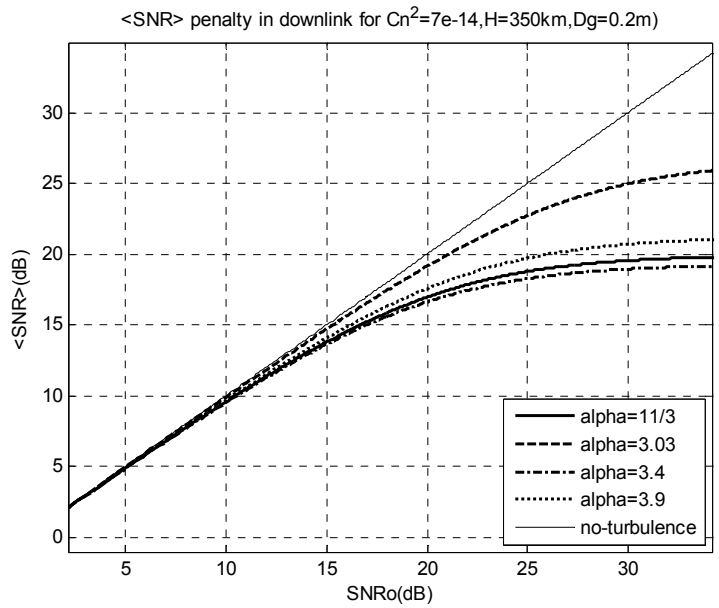

Figure 5-Mean Signal to Noise (dB unit) as a function of no-turbulence Signal to Noise ratio (dB unit) for different alpha values for downlink path

6.2 Uplink: spherical model

We plot the Mean Signal to Noise Ratio as a function of signal to noise ratio without turbulence for several alpha values using spherical wave model for scintillation (11). We take

$$H = 350km; h_0 = 0; \varsigma = 0; \tilde{C}_n^2(0) = 7 \cdot 10^{-14}\, m^{-\alpha+3}; \lambda = 1.55\mu m; D_G = 0.1m.$$

The plot is shown in figure 6.

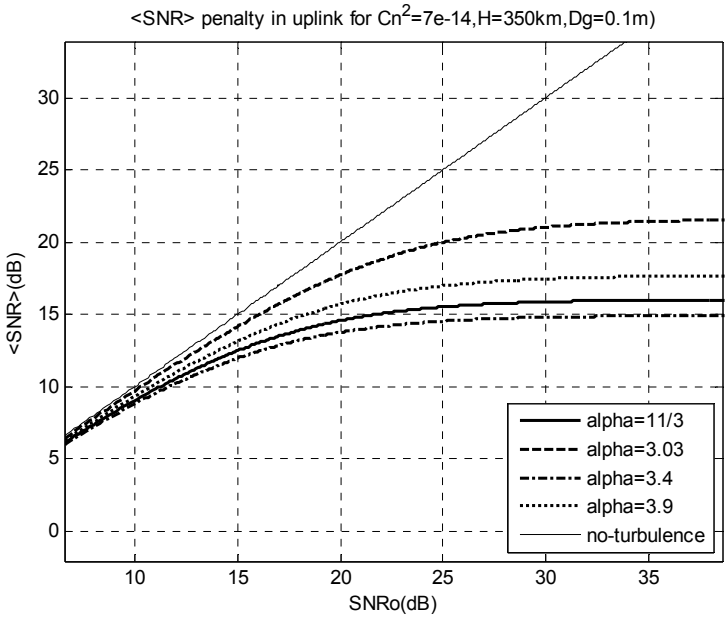

Figure 6 -Mean Signal to Noise (dB unit) as a function of no-turbulence Signal to Noise ratio (dB unit) for different alpha values for uplink

7. MEAN BIT ERROR RATE

In the presence of optical turbulence, the probability of error is considered a conditional probability that must be averaged over the PDF of the random signal to determine the unconditional mean BER. In terms of a normalized signal with unit mean, this leads to the expression [1]

$$\Pr(E) = \langle BER \rangle = \frac{1}{2} \cdot \int_0^\infty p_I(u) \cdot erfc\left(\frac{\langle SNR \rangle \cdot u}{2 \cdot \sqrt{2}} \right) du, \tag{15}$$

where $p_I(u)$ is taken to be the log normal distribution with unit mean [1][13].

7.1 Downlink: plane wave model

We plot the Mean Bit Error Rate as a function of $\langle SNR \rangle$ for several alpha values using the plane wave model for scintillation (9).
We take the same parameters

$$H = 350km; h_0 = 0; \varsigma = 0; \tilde{C}_n^2(0) = 7 \cdot 10^{-14} m^{-\alpha+3}; \lambda = 1.55\mu m; D_G = 0.2m.$$

The plot is shown in figure 7

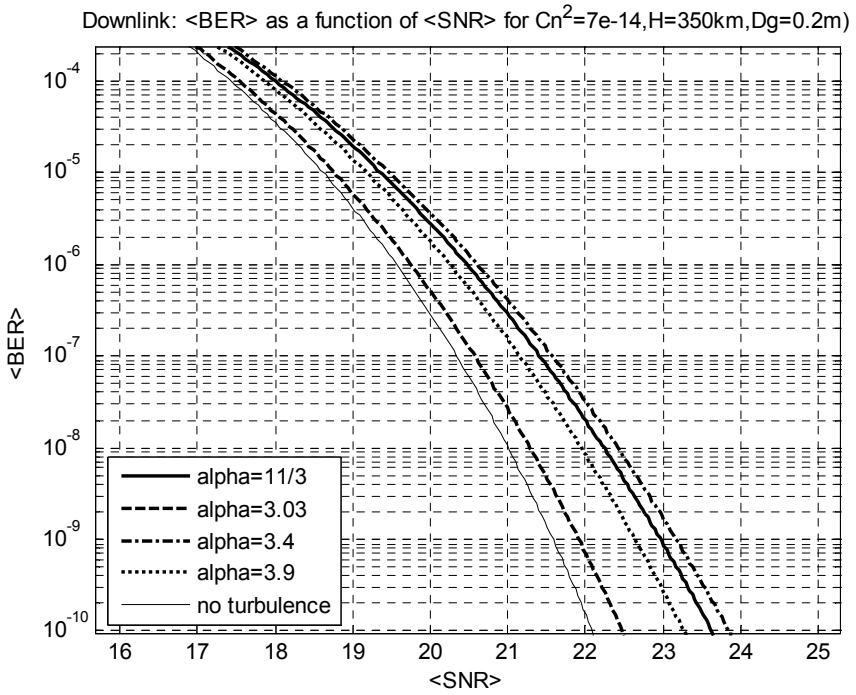

Figure 7 – Mean Bit Error Rate (BER) as a function of Mean Signal to Noise ratio for different alpha values for downlink path

It is shown the impact of the alpha variation on $\langle BER \rangle$ performance. Also in this analysis when alpha is lower than $\alpha = 11/3$ there is a penalty, but for alpha higher than $\alpha = 11/3$ there is a improvement on the system performance.

However when alpha assumes values close to $\alpha = 3$ there is a gain on the $\langle BER \rangle$ performance with respect to $\langle BER \rangle$ value correspondent to $\alpha = 11/3$ because the scintillation approaches zero.

7.2 Uplink: spherical wave model

We plot the Mean Bit Error Rate as a function of $\langle SNR \rangle$ for several alpha values using the spherical wave model for scintillation (11). We take the same parameters

$H = 350km; h_0 = 0; \varsigma = 0; \tilde{C}_n^2(0) = 7 \cdot 10^{-14} m^{-\alpha+3}; \lambda = 1.55\mu m; D_G = 0.1m.$

The plot is shown in figure 8.

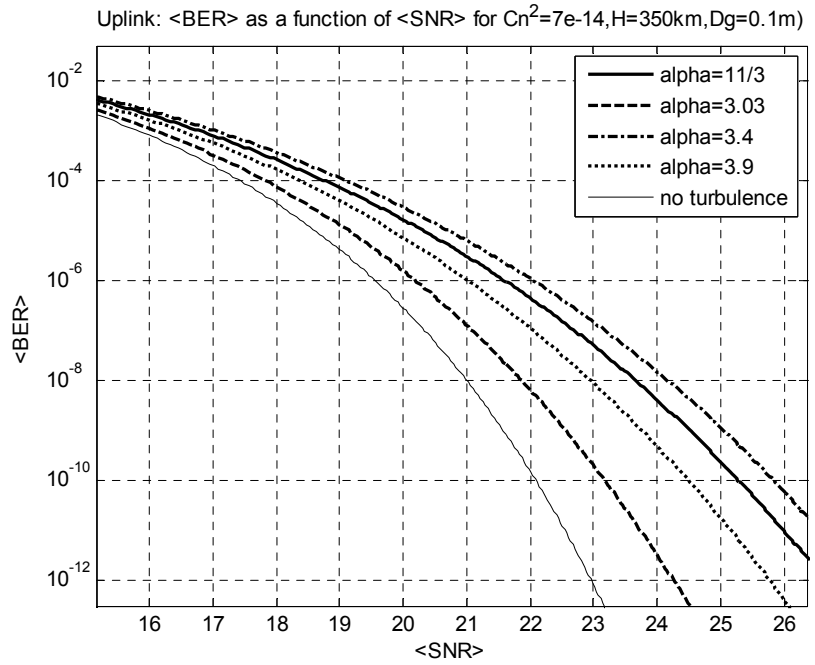

Figure 8 – Mean Bit Error Rate (BER) as a function of Mean Signal to Noise ratio for different alpha values for uplink path

From the figure above we deduce the same considerations of downlink case.

8. DISCUSSION

In this paper we have introduced a non-Kolmogorov power spectrum which uses both a generalized exponent and a generalized amplitude factor instead of a constant standard exponent value $\alpha = 11/3$ and a constant amplitude factor 0.033 associated with the conventional Kolmogorov spectrum. This non-Kolmogorov spectrum has been developed from a generalized structure function. It has been shown, for uplink and downlink paths, the *beam spread*, *Scintillation*, *Probability of fade*, *mean SNR* and *mean BER* as variations depending on the alpha exponent lead to results somewhat different than obtained with the standard value of Kolmogorov $\alpha = 11/3$.

For uplink and downlink, it has been shown that for alpha values lower than $\alpha = 11/3$, but not for alpha close to $\alpha = 3$, there is a remarkable increase of scintillation and consequently a major penalty on the system performance. However when alpha assumes a value close to $\alpha = 3$ the amplitude factor $A(\alpha)$ assumes a very low value and

consequently the *long term beam spread* and *scintillation* decrease leading an improvement on the system performance. Finally also for alpha values higher than $\alpha = 11/3$ the *scintillation* decreases and consequently it improves the system performance.

9. REFERENCES

1. Larry C. Andrews, Ronald L. Phillips. *Laser Beam Propagation through Random Media*. Spie Press, second edition - 2005.
2. Larry C. Andrews, Ronald L. Phillips, Cynthia Y. Hopen. *Laser Beam Scintillation with Applications*. Spie Press, 2001.
3. David Dayton, Bob Pierson, Brian Spielbusch. *Atmospheric structure function measurements with a Shack-Hartmann wave front sensor.* Optics letters ,vol.17, num. 24,1992.
4. J. McWilliam, Phys. Fluids, A 2, 547, 1990.
5. Mikhail S. Be1enkii, Stephen J. Karis, James M. Brown II, and Robert Q. Fugate. *Experimental study of the effect of non-Kolmogorov stratospheric turbulence on star image motion.* SPIE vol. 3126, 1997.
6. Ephim Golbraikh, Norman S. Kopeika. *Behavior of structure function of refraction coefficients in different turbulent fields.* Applied Optics, vol 43, num. 33, 2004.
7. Gregory Falkovich, Katepalli R. Sreenivasan. *Lessons from Hydrodynamic Turbulence*. Physics Today, April 2006.
8. A I Kon. *Qualitative theory of amplitude and phase fluctuations in a medium with anisotropic turbulent irregularities.* Wave in random media 4, 297-305, 1994.
9. Bruce E. Stribling, Byron M. Welsh and Michael C. Roggemann. *Optical propagation in non-Kolmogorov Atmospheric Turbulence.* SPIE vol.2471, 181-196, 1995.
10. Demos T. Kyrazis, John Wissler, Donna D.B. Keating, Amanda J.Preble, Kenneth P. Bishop. *Measurement of optical turbulence in the upper troposphere and lower stratosphere.* SPIE vol. 2110, 1994.
11. Mikhail S. Belen'kii, Stephen J.Karis, Christian L. Osmon. *Experimental evidence of the effects of non-Kolmogorov turbulence and anisotropy of turbulence.* SPIE vol. 3749, 1999.
12. Robert R. Beland, *Some aspects of propagation through weak isotropic non-Kolmogorov turbulence.* SPIE vol. 2375, 1995.
13. Italo Toselli, Larry C. Andrews, Ronald L. Phillips. *Free space optical system performance for laser beam propagation through non Kolmogorov turbulence*. SPIE vol. 6457, 2007.